Manufacturing Technologies and Applications
MATECA

Improvement in Surface and Tribological Properties of Fe-1%C Steel Produced by Powder Metallurgy Method by Thermal Spray Coating

Gözde Altuntaş[1],*

[1]*Gazi University, Faculty of Technology, Department of Metallurgical and Materials Engineering, Ankara, Turkey*
** Corresponding author's e-mail address: gozdealtuntas@gazi.edu.tr*

ABSTRACT

In this study, the surface properties of Fe–1wt.%C based components produced by powder metallurgy (P/M) were enhanced using a NiCrBSi alloy deposited via the Powder Flame Spray (PFS) technique. Detailed examinations revealed that the inherent surface roughness of the P/M substrates promoted strong mechanical interlocking between the molten spray droplets and the substrate. X-ray diffraction (XRD) analyses confirmed the formation of Cr_2B (chromium boride) and various nickel–chromium silicide phases (Cr_3Ni_2Si and $Cr_3Ni_5Si_2$), which developed as a result of the rapid solidification occurring during the spraying process. Microhardness measurements indicated a significant increase in surface hardness from approximately 250 HV for the uncoated substrate to about 550 HV after coating, corresponding to an improvement of nearly 110%. This hardness level exceeds the conventional benchmark value of 40 HRC (≈400 HV), demonstrating that superior mechanical performance can be achieved through spray-induced energy transfer even in the absence of post-deposition heat treatment. Tribological evaluations showed that the coefficient of friction (COF), which ranged between 0.8 and 1.0 for the uncoated surface, was markedly reduced to approximately 0.2 with a coating thickness of 150 µm. Scanning electron microscopy (SEM) observations revealed severe material loss and deep abrasive grooves on the uncoated samples, whereas the NiCrBSi-coated surfaces maintained structural integrity owing to the presence of hard intermetallic phases, resulting in a more stable and improved wear regime. Overall, the results demonstrate that high wear resistance and low friction performance can be effectively achieved in powder metallurgy components through appropriate coating parameters, without the need for additional heat treatment.

Keywords: *Thermal spray coating, powder flame spray, NiCrBSi, tribology, powder metallurgy,*

Toz Metalurjisi Yöntemiyle Üretilen Fe-1%C Çeliğinin Yüzey ve Tribolojik Özelliklerinin Termal Püskürtme Kaplama Yöntemiyle İyileştirilmesi

ÖZET

Bu çalışmada, toz metalurjisi (P/M) ile üretilen Fe–1wt.%C bazlı bileşenlerin yüzey özellikleri, Toz Alev Püskürtme (PFS) tekniğiyle kaplanmış bir NiCrBSi alaşımı kullanılarak iyileştirilmiştir. Detaylı incelemeler, P/M alt tabakalarının doğal yüzey pürüzlülüğünün, erimiş püskürtme damlacıkları ile alt tabaka arasında güçlü mekanik kenetlenmeyi teşvik ettiğini ortaya koymuştur. X-ışını kırınımı (XRD) analizleri, püskürtme işlemi sırasında meydana gelen hızlı katılaşma sonucu oluşan Cr_2B (krom borür) ve çeşitli nikel-krom silisit fazlarının (Cr_3Ni_2Si ve $Cr_3Ni_5Si_2$) oluşumunu doğrulamıştır. Mikro sertlik ölçümleri, kaplamasız alt tabaka için yaklaşık 250 HV olan yüzey sertliğinin, kaplamadan sonra yaklaşık 550 HV'ye yükseldiğini ve yaklaşık %110'luk bir iyileşme sağladığını göstermiştir. Bu sertlik seviyesi, geleneksel 40 HRC (≈400 HV) referans değerini aşarak, kaplama sonrası ısıl işlem olmaksızın bile püskürtme kaynaklı enerji transferi yoluyla üstün mekanik performans elde edilebileceğini göstermektedir. Tribolojik değerlendirmeler, kaplamasız yüzey için 0,8 ile 1,0 arasında değişen sürtünme katsayısının (COF), 150 µm kaplama kalınlığı ile yaklaşık 0,2'ye önemli ölçüde düştüğünü göstermiştir. Taramalı elektron mikroskobu (SEM) gözlemleri, kaplamasız numunelerde ciddi malzeme kaybı ve derin aşındırıcı oluklar ortaya koyarken, NiCrBSi kaplı yüzeyler, sert intermetalik fazların varlığı sayesinde yapısal bütünlüğünü koruyarak daha kararlı ve gelişmiş bir aşınma rejimi sağlamıştır. Genel olarak, sonuçlar, uygun kaplama parametreleri ile toz metalurjisi bileşenlerinde ek ısıl işleme gerek kalmadan yüksek aşınma direnci ve düşük sürtünme performansının etkili bir şekilde elde edilebileceğini göstermektedir.

Anahtar Kelimeler*: Termal sprey kaplama, toz alev sprey, NiCrBSi, triboloji, toz metalurjisi,*

1. INTRODUCTION

Low-alloy high-strength steels have proved to be important materials in oil and gas, construction and mechanical sector because of their low cost and good combination of strength, ductility, and toughness [1-2]. Powder-metallurgical (P/M) sintered parts are readily used as precision parts in many industrial sectors,

*Corresponding author, e-mail: gozdealtuntas@gazi.edu.tr

Received 08.01.2026; Accepted 13.04.2026
https://doi.org/10.52795/mateca.1859575
To cite this article: G. Altuntas, Improvement in Surface and Tribological Properties of Fe-1%C Steel Produced by Powder Metallurgy Method by Thermal Spray Coating, Manufacturing Technologies and Applications 7(1)(2026) 34-42.

especially in engines and transmissions [3-4]. Components produced by conventional powder metallurgy typically exhibit limited resistance to dynamic loading due to the inherent porosity within their microstructure [5-6]. Consequently, these parts are commonly subjected to post-sintering treatments such as heat treatment [7], surface hardening [8], or surface coating [9-10] to enhance their mechanical and tribological performance for engineering applications. Among modern surface engineering techniques, thermal spray coatings are widely preferred for enhancing the surface properties of industrial components, providing protection against wear, corrosion, and high-temperature oxidation [11]. Among these, NiCrBSi (Nickel–Chromium–Boron–Silicon) alloys possess strategic importance due to their self-fluxing capability and multifunctional protective characteristics [12]. The primary purpose of NiCrBSi coatings is to increase the surface hardness of the substrate material typically low-alloy steels and to extend component service life under severe operating conditions. Within the alloy, chromium (Cr) contributes to corrosion resistance by forming a dense chromium oxide layer on the surface, whereas boron (B) and silicon (Si) lower the melting temperature and act as fluxing agents during deposition [13]. This facilitates the formation of a dense, metallurgically bonded coating after the post-deposition fusing treatment [14]. NiCrBSi coatings applied via high-velocity oxy-fuel (HVOF) or plasma spray processes demonstrate excellent wear resistance, attributed to the presence of hard boride and carbide phases [15]. Consequently, these coatings have become a preferred choice for the protection of shafts, valves, pump components, and extrusion screws in critical sectors such as aerospace, energy, petrochemical, and automotive industries. Among the various deposition techniques, the Powder Flame Spray (PFS) process plays a dominant role in the industrial application of self-fluxing NiCrBSi coatings due to its operational flexibility and cost-effectiveness [16]. A key advantage of this technique is that both deposition and subsequent remelting (fusing) can be performed using the same equipment or within an integrated setup, enabling the coating to establish not only a mechanical but also a metallurgical bond with the substrate a critical requirement for components operating under high loads [17]. Flame spray coating offers lower investment and maintenance costs compared to other thermal spray coating methods (such as HVOF or Plasma), enabling on-site coating of large-scale industrial parts [18]. During the application of NiCrBSi powders with this method, the powder particles are heated homogeneously thanks to the low flame rate and controllable heat input. This, combined with the oxide-dissolving ability of Boron (B) and Silicon (Si) elements, ensures minimum porosity and maximum density in the coating layer [19]. In addition, the powder flame spray method minimizes raw material waste by providing high material transfer efficiency on parts with complex geometries. The combination of this method with NiCrBSi alloys offers one of the solutions for the economical refurbishment and protection of large-surface components exposed to wear, especially in the mining, agriculture, and energy sectors [19,20].

Although NiCrBSi-based coatings are frequently investigated in the literature in conjunction with post-deposition remelting (fusing) treatments, such thermal processes may induce distortion and microstructural alterations in the substrate, which can be restrictive for certain industrial applications. This issue is particularly critical for Fe–C based components produced via powder metallurgy (P/M), where secondary high-temperature treatments (fusing) can adversely affect dimensional stability and matrix properties. The present study aims to investigate the as-sprayed performance of NiCrBSi coatings deposited by the Powder Flame Spray (PFS) technique onto Fe–C alloys manufactured by powder metallurgy, without the application of any subsequent heat treatment. Specifically, the work comprehensively examines, for the first time, the influence of the surface porosity of the P/M substrate on the mechanical interlocking mechanism of non-fused NiCrBSi particles and the resulting wear behaviour of the as-sprayed coating layer.

2. MATERIAL AND METHOD

For the production of high-carbon powder metallurgy (P/M) steel, high-purity (99.9%) water-atomized iron powders (Nanografi®) with an average particle size of 325 mesh were mixed with 1.0 wt.% high-purity (99.9995%) graphite powders (Alfa Aesar®) having an average particle size of 200 mesh. A lubricant of zinc stearate (0.5 wt.%) was incorporated into the powder mixture, which was subsequently blended for 30 minutes using a 3D Turbula® mixer to ensure homogeneous distribution. The powder mixtures were uniaxially compacted at room temperature under a pressure of 800 MPa using a single-acting hydraulic press to form green compacts following the ASTM G99 standard. Subsequently, the compacts were sintered at 1280 °C for 30 minutes under a vacuum of 5×10^{-2} Pa. Following the sintering process, the carbon content of the alloy was quantitatively analyzed using a Bruker Q4 Tasman Advanced CCD-based Optical Emission Spectrometer® and was found to be 1.0 wt.%. In accordance with ASTM B962-17, the densities of both the pressed and sintered specimens were measured using Archimedes' principle with an A&D HR-250AZ® analytical balance, resulting in values of 6.94 g/cm³ and 7.38 g/cm³, respectively. Microstructural examinations were performed using a JEOL JSM-6060LV® scanning electron microscope (SEM). Before SEM observation, the specimens

underwent conventional metallographic preparation followed by etching with a 3% nital solution (3 mL HNO_3 and 97 mL ethanol). Prior to coating, the sample surfaces were sandblasted in a pressurized blasting chamber. Subsequently, coating was applied with a 50 µm powder mixture of NiCrBSi at a powder feed rate of 10 g/min. Coating thickness measurements vary depending on the number of passes of the torch used for coating. The coating powder mixture consists of 17% Cr, 4% Si, 3% B, and the balance is Ni. A coating thickness of 50 µm was obtained in a single pass at a feed rate of 10 g/min. The flame characteristic was adjusted with an O_2/C_2H_2 ratio of approximately 2:1; oxygen and acetylene flow rates were kept around ~40 and ~35 L/min, respectively. After coating, surface thickness measurements were taken using a mini test 650 device. To identify the alloy phases formed by compounds precipitated after surface coating, X-ray diffraction (XRD) analysis was carried out using a Bruker D8 Advance® diffractometer equipped with a Cu Kα radiation source ($\lambda = 0.154$ nm) and a step size of 0.06°/s. The microhardness (HV0.1) of the samples was measured in accordance with ASTM E384 using a Qness 60 M EVO® microhardness tester with a diamond indenter and an applied load of 0.1 kgf. Dry sliding wear tests were conducted using the pin-on-disk method in accordance with the ASTM G99 standard. The tests were performed under a constant load of 10 N, at a sliding speed of 1 m/s, over a sliding distance of 1000 m, and at room temperature using a UTS Tribometer device.

3. RESULTS AND DISCUSSION

As shown in Figure 1, and as described in the Experimental Studies section, the SEM microstructure of the metallographically prepared specimen for metallurgical characterisation is presented. Examination of the microstructure reveals that the plain high-carbon steel consists of the conventional microstructural constituents of primary cementite (indicated by dashed yellow lines) and dense lamellar pearlite colonies (indicated by dashed red lines). In addition, surface-connected pores (highlighted with blue circles), which represent one of the inherent drawbacks of conventional powder metallurgy production, are heterogeneously distributed within the microstructure [21]. A detailed investigation of the microstructure in Figure 1 shows no evidence of local decarburisation, confirming that the sintering process of the alloy was successfully performed in an isolated environment. The primary cementite phase, possessing an orthorhombic crystal lattice, appears as a continuous network within the microstructure, exhibiting a hard and brittle nature. These primary cementites, which enhance the hardness of the alloy, act as stress concentrators under mechanical loading and vibrational effects, thereby increasing brittleness [22]. Furthermore, numerous pearlite lamellae with varying angular orientations characteristic of hypereutectoid steels are also observed abundantly throughout the structure.

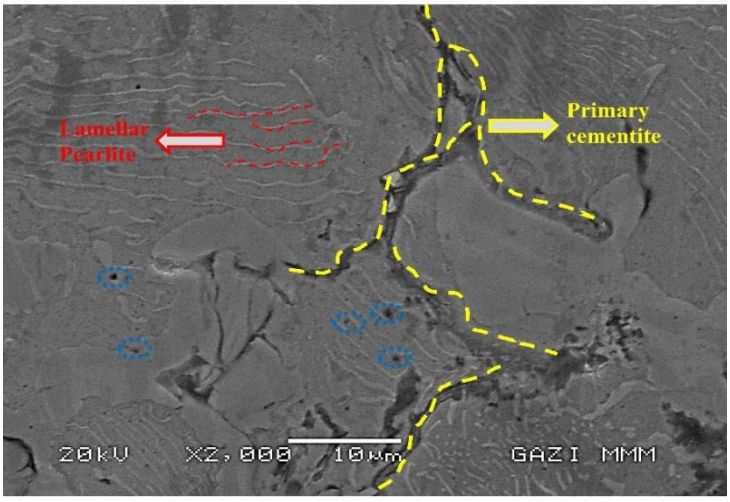

Figure 1. SEM micrograph of the Fe–1%C alloy following the sintering process.

It is well established that the inherent pores originating from the production process reduce hardness and serve as initiation sites for cracks, thereby adversely affecting various static and dynamic mechanical properties. However, the microchannels formed by surface-connected pores enhance tribological performance on frictional surfaces by facilitating lubricant retention [23]. Figure 2 presents the microstructure and EDS analysis of the coated surface following sandblasting of the fabricated specimens. Regions where powder particles have impacted and spread over the surface (splats) are visible. Nevertheless, instead of exhibiting

complete melting, the coating predominantly displays a “semi-molten” morphology, where the particles have largely retained their original shape. The EDS results indicate the elemental composition of the Ni–Cr–B–Si blended powder. Due to the small atomic radius of boron (B), its quantitative detection in EDS analyses is challenging; therefore, the SEM spot size was increased up to 60 to ensure the detection of boron within this range.

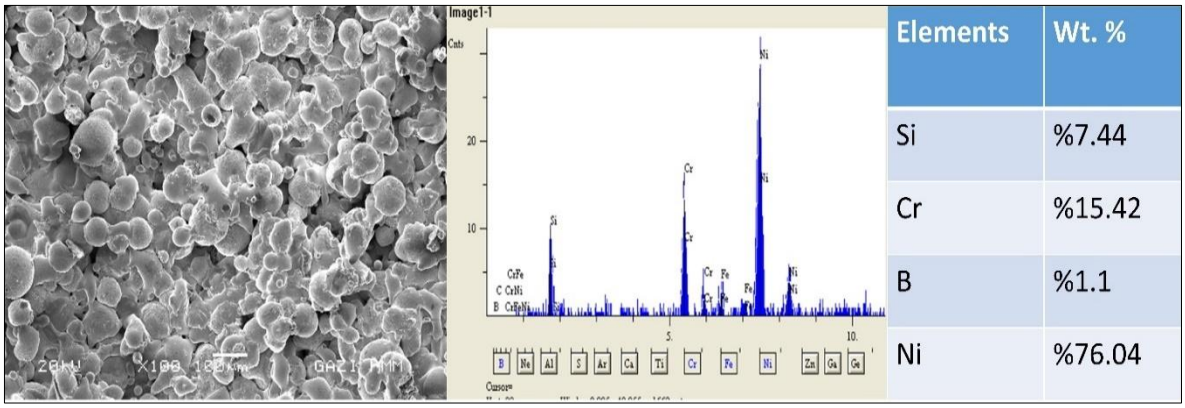

Elements	Wt. %
Si	%7.44
Cr	%15.42
B	%1.1
Ni	%76.04

Figure 2. SEM image and EDS analysis of the coating surface.

Figure 3 presents the SEM micrographs obtained from the cross-section of the coated specimens, illustrating the interfacial relationship and coating porosity. To achieve full densification and transform the bonding into a metallurgical joint, the coating material typically requires a post-deposition heat treatment. In the literature, this process for NiCrBSi alloys is commonly referred to as “fusing” or “remelting”, which is generally carried out at approximately 1000 °C. At such temperatures, the Fe–C substrate alloy transitions into the austenitic phase, resulting in grain growth. Therefore, to preserve the structural integrity of the substrate and to retain the advantages of powder metallurgy, no post-coating heat treatment was applied. The boron (B) and silicon (Si) elements present in the NiCrBSi alloy facilitate the removal of surface oxides during the spraying process, thereby improving wettability and enabling interfacial adhesion even in the absence of heat treatment [11]. The SEM micrographs reveal that the interfacial bonding quality is satisfactory; although heat treatment typically enhances densification and metallurgical bonding, the high surface energy and roughness inherent to the powder metallurgy substrate provide a sufficient foundation for maintaining a continuous mechanical bond [24].

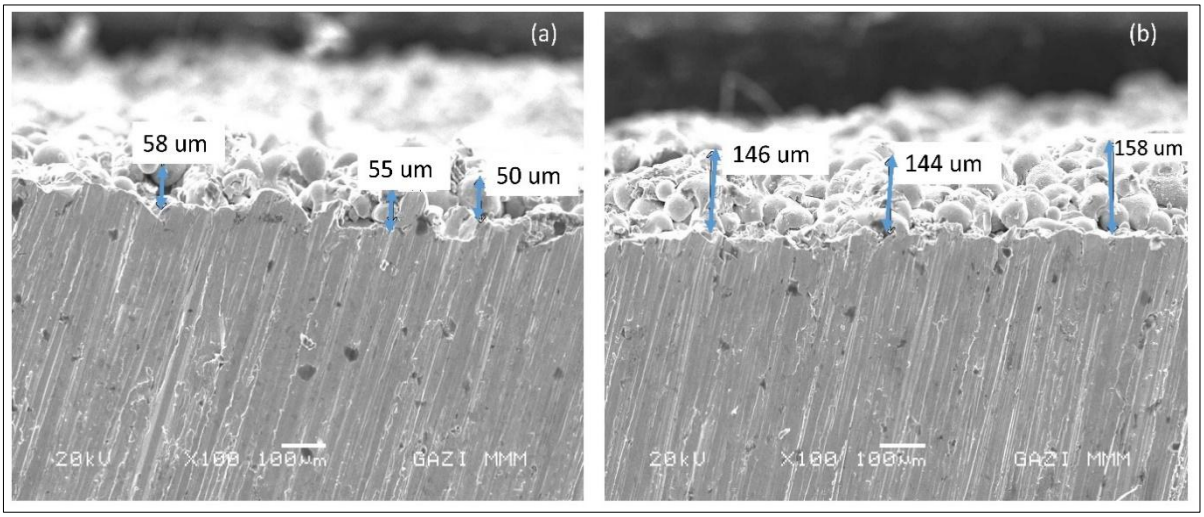

Figure 3. SEM images of the base material/coating interface in cross-section of the samples. (a) 50 µm coating (b) 150 µm coating.

Figure 4 presents the XRD patterns of coated specimens. The following card numbers were used in determining the phases and compounds by X-ray analysis: PDF 00-054-0369 Cr3Ni2Si, PDF 01-071-4653 Ni, PDF 01-089-2731 Cr3Ni5Si2, PDF 00-038-1399 Cr2B, PDF 01-087-0721 Fe, and PDF 01-081-4937 Cr. The Fe peak originating from the Fe–C substrate is still detectable even from the coating surface. In the powder flame spray process, the feedstock powders impact the substrate in a semi-molten state within the oxy-acetylene flame. The high temperature of the flame provides sufficient energy for the particles to react both during their flight and upon impact. Owing to its self-fluxing nature, the NiCrBSi alloy exhibits a relatively low melting point, which promotes compound formation. Upon impact, the molten droplets experience extremely rapid cooling, supplying the driving force necessary for atomic bonding and the formation of new crystalline phases. Consequently, chromium (Cr) and nickel (Ni) are detected both as individual phases and as compounds in combination with silicon (Si) and boron (B) [11, 25]. Even in the absence of post-deposition heat treatment, the spray process itself acts as a miniature reactor, facilitating the formation of these hard phases. The presence of such phases indicates that the coating is not only mechanically adhered to the substrate but also chemically integrated. As coating thickness increases, the intensity of the substrate-related Fe peaks decreases, whereas the intensity of Ni–Cr peaks increase, confirming the progressive dominance of the coating layer.

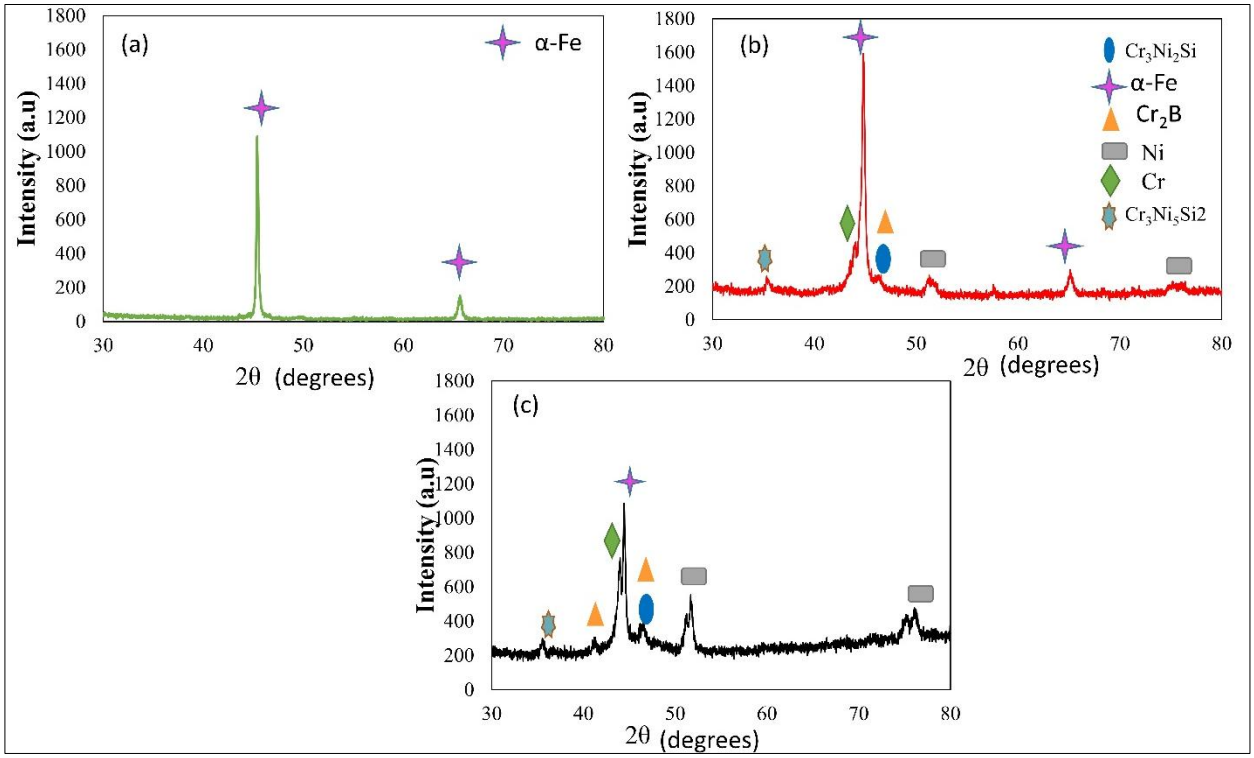

Figure 4. XRD graphs of the samples (a) Fe-C alloy (b) 50 µm coating (c) 150 µm coating

Figure 5 presents the SEM micrographs and three-dimensional profilometry images of the samples after the wear tests. As shown in Figure 5(c), the uncoated material exhibits severe wear damage characterised by a wide and deep wear track. Pronounced and elongated wear grooves are clearly observed, indicating an aggressive abrasive wear mechanism. This behaviour confirms that the Fe–C substrate is significantly softer than the NiCrBSi coating and is therefore more readily ploughed by the counterface during sliding contact [26]. The advanced degree of surface degradation observed on the uncoated sample clearly demonstrates the necessity of surface coating for improving wear resistance. Despite the absence of any post-deposition heat treatment, the NiCrBSi coating did not exhibit spallation or delamination during wear testing. This observation highlights the effectiveness of mechanical interlocking between the coating and the substrate, as well as the strong interfacial bonding promoted by rapid solidification and phase formation during the spraying process. In contrast, Figures 5(a) and 5(b) show that the original surface topography of the coated samples remains largely preserved after wear testing. The rounded surface features correspond to partially molten NiCrBSi powder particles deposited during spraying. Although slight surface flattening is observed in the region

indicated by the yellow arrow, the coating appears largely intact, indicating that significant material removal has not yet occurred.

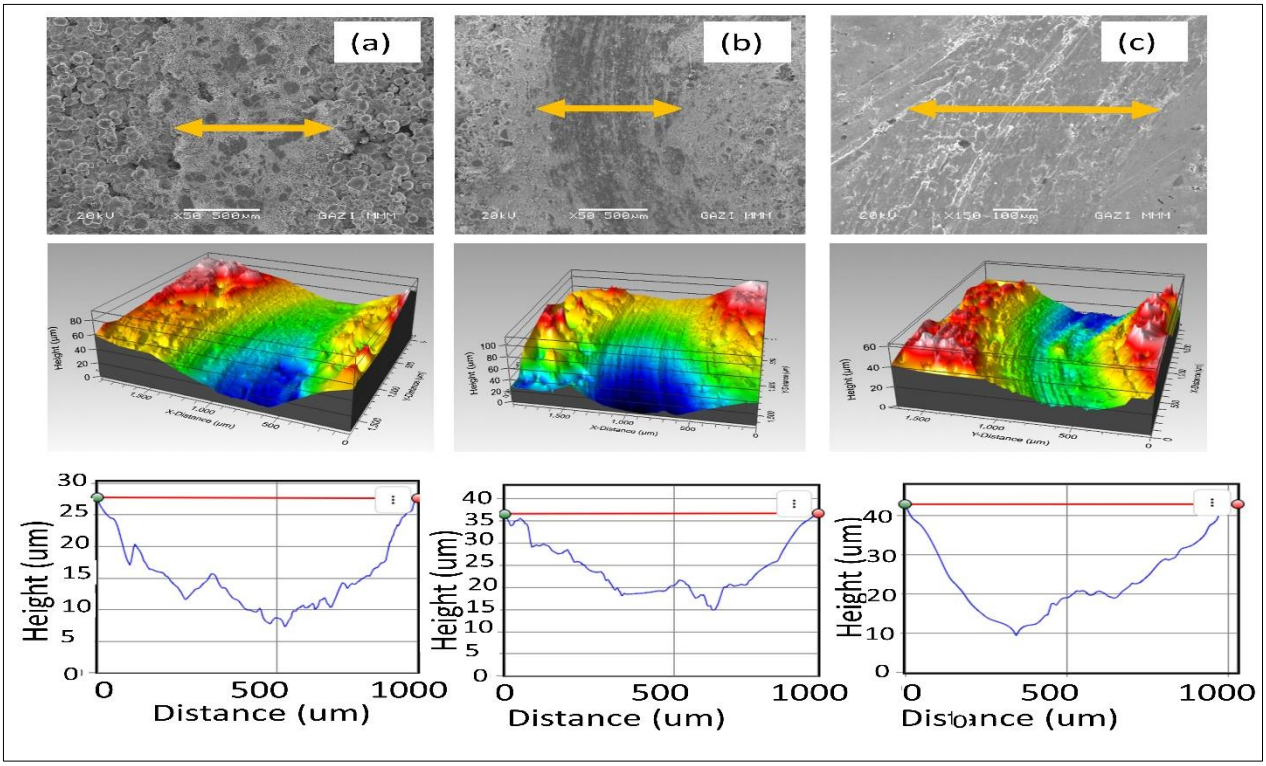

Figure 5. SEM and 3D profilometer images of the samples after wear testing (a) 150 µm coating (b) 50 µm coating (c) Fe-C alloy

Figure 6(a-b) shows the wear coefficient and friction coefficient graphs of the samples. The dry sliding wear resistance of the NiCrBSi-coated powder metallurgy steel samples was quantitatively evaluated by calculating the wear coefficient based on the Archard equation [27] (Equation 1). The variation in wear coefficients obtained from the pin-on-disc wear tests for each sample is illustrated in Figure 6a, providing a comparative assessment of the coating's tribological performance.

$$v/Ns=K \qquad \text{Eq. 1}$$

where v denotes the volumetric material loss at the contact surface (m^3), s is the sliding distance (m), K represents the specific wear coefficient ($m^3\ N^{-1}\ m^{-1}$), and N is the applied normal load (N).
As inferred from the wear coefficient graph, the sintered uncoated material exhibited a wear coefficient of $0.78 \times 10^{-15}\ m^3\ N^{-1}\ m^{-1}$. In contrast, a pronounced reduction in the wear coefficient was observed for the coated samples, with values of $0.16 \times 10^{-15}\ m^3\ N^{-1}\ m^{-1}$ and $0.12 \times 10^{-15}\ m^3\ N^{-1}\ m^{-1}$ for coating thicknesses of 50 µm and 150 µm, respectively. From a metallurgical perspective, the relatively high wear coefficient of the uncoated powder metallurgy steel can be attributed to the fact that, during wear testing, the applied normal load is predominantly supported by the Fe-based matrix, which possesses a significantly lower hardness compared to the NiCrBSi-coated surface [28]. In addition, the presence of inherent isolated and open porosity within the sintered structure, which reduces the effective density of the alloy, promotes stress concentration during sliding contact. These stress concentration sites facilitate microcrack initiation and particle detachment, thereby accelerating material removal. In contrast, the NiCrBSi-coated P/M steel samples with coating thicknesses of 50 µm and 150 µm exhibited substantially lower wear coefficients. This behaviour can be ascribed to the presence of hard boride and silicide phases and a dense microstructural morphology, which collectively reduce the real contact area and restrict plastic deformation at the sliding interface. Consequently, material removal is significantly suppressed, leading to improved wear resistance and lower wear coefficients [29]. Conversely, the absence of such reinforcing phases and microstructural integrity in the uncoated powder metallurgy steel causes these parameters to act in a wear-accelerating manner.

The coefficient of friction (COF) results further elucidates the tribological performance of the NiCrBSi coating and the influence of coating thickness. The uncoated Fe–C alloy exhibited a consistently high COF, ranging between 0.8 and 1.0. The approximately 50% reduction in COF observed for the 50 µm thick coating is attributed to the presence of hard intermetallic phases identified by XRD, which enhance load-bearing capacity and stabilise the sliding contact. At a coating thickness of 150 µm, the mechanical contribution of the Fe–C substrate becomes less pronounced, while the intrinsic tribological characteristics of the NiCrBSi alloy dominate the contact behaviour. This thickness is sufficient to act as an effective barrier against direct substrate wear, thereby providing enhanced protection of the base material and further stabilising the frictional response.

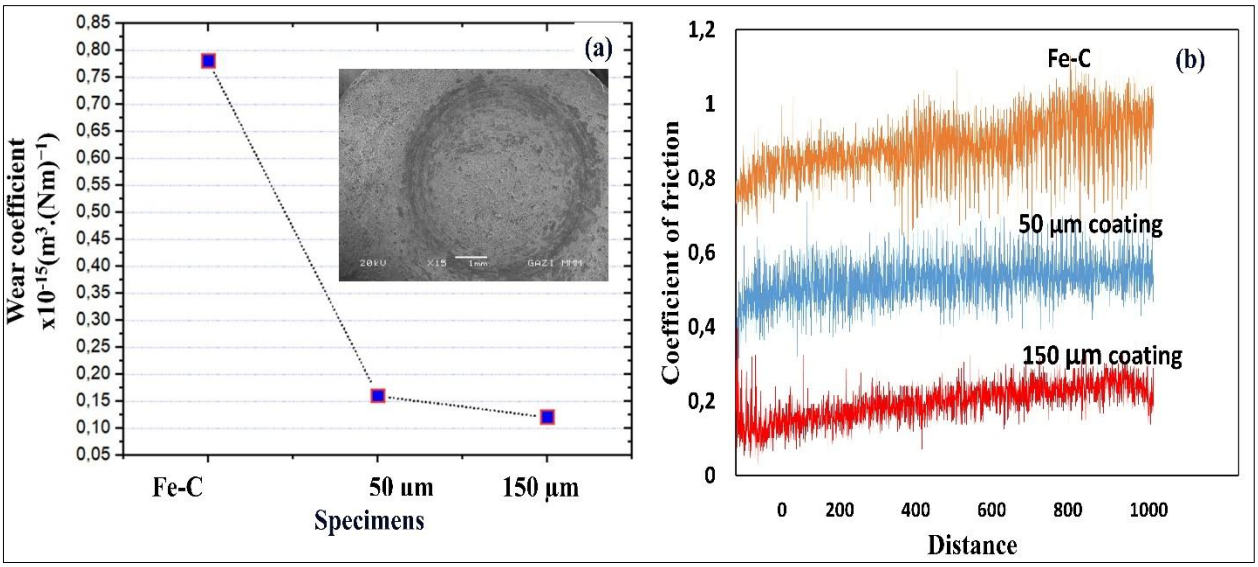

Figure 6. Graphs of (a) coefficient of wear and (b) coefficient of friction after wear testing of the samples.

Table 1 summarises the cross-sectional hardness values measured across the substrate, interfacial region, and coating. A pronounced increase in hardness, exceeding a twofold rise from approximately 250 HV in the substrate to about 550 HV in the coating, is observed, clearly demonstrating the effectiveness of the Powder Flame Spray process. The obtained hardness level of 550 HV is due to the absence of reheating after coating. Literature shows that when remelting/fuse heat treatment is applied after coating, hardness levels of 700-800 HV are measured [30,31]. This enhanced hardness is primarily attributed to the formation of hard intermetallic phases. In particular, the presence of chromium borides and nickel silicides identified by XRD analyses, combined with the rapid solidification mechanisms inherent to the spraying process, plays a critical role in strengthening the coating microstructure and improving its load-bearing capacity [12,30].

Table 1. Cross-sectional microhardness measurements obtained from the base material through the interfacial region to the coating.

	Fe-%1C alloy	Interface	Coating Area
Hardness HV0.1	250-242-248-255-253 ±5	380-410-412-390-398 ±14	565-568-550-540-538 ±14

4. CONCLUSIONS

In this study, NiCrBSi coatings were successfully deposited onto Fe–C alloys produced via the powder metallurgy route using the Powder Flame Spray (PFS) technique. The key findings can be summarised as follows:

- The inherent porosity of the powder metallurgy substrates provided an ideal anchoring surface for the molten NiCrBSi droplets, ensuring strong mechanical interlocking without the need for post-deposition heat treatment.
- XRD analyses confirmed the formation of hard and stable intermetallic phases on the surface, promoted by the rapid cooling rates inherent to the spray process.

- The coefficient of friction of the uncoated Fe–C alloy, which reached approximately 1.0, showed a remarkable reduction after NiCrBSi coating. In particular, the 150 μm-thick coating exhibited the most stable wear resistance, lowering the coefficient of friction to around 0.2.
- SEM observations revealed severe abrasive grooves and material loss on the uncoated surfaces, whereas the coated samples demonstrated that hard boride and silicide phases bore the applied loads, preserving surface integrity and improving the wear regime.
- Microhardness measurements indicated an average hardness of 250 HV 0.1 for the base material and 550 HV 0.1 for the coating layer.

REFERENCES

[1] C. Gao, M.Q. Yang, J.C. Pang, S.X. Li, M.D. Zou, X.W. Li, Z.F. Zhang, Abnormal relation between tensile and fatigue strengths for a high-strength low-alloy steel, Mater Sci Eng A 832 (2022) 142418. https://doi.org/10.1016/j.msea.2021.142418

[2] O. Bouaziz, H. Zurob, M. Huang, Driving force and logic of development of advanced high strength steels for automotive applications, Steel Res Int 84 (2013) 937–947. https://doi.org/10.1002/srin.201200288

[3] P. Skoglund, O. Litstrom, A. Flodin, Improvement of powder metallurgy gears for engines and transmissions, SAE Technical Paper (2013). https://doi.org/10.4271/2013-32-9102

[4] P. Ramakrishnan, Automotive applications of powder metallurgy, in: I.T.H. Chang, Y. Zhao (Eds.), Advances in Powder Metallurgy, Woodhead Publishing, Oxford, 2013, pp. 493–519. https://doi.org/10.1533/9780857098900.4.493

[5] H. Danninger, C. Gierl, Powder metallurgy steels for highly loaded precision parts, Int J Mater Prod Technol 28 (2007) 338–348. https://doi.org/10.1504/IJMPT.2007.013084

[6] H. Danninger, M. Dlapka, Heat treatment of sintered steels – what is different, HTM J Heat Treat Mater 73 (2018) 117–130. https://doi.org/10.3139/105.110353

[7] O. Altuntaş, Crystallographic analysis of a new heat treatment strategy for improving the mechanical properties of powder metallurgical steel, Can Metall Q 63 (2024) 1061–1069. https://doi.org/10.1080/00084433.2023.2251215

[8] T.H. Lim, C.S. Lee, I.S. Cho, A. Amanov, Better surface integrity and tribological properties of steel sintered by powder metallurgy, Materials 13 (2020) 3172. https://doi.org/10.3390/ma13143172

[9] D. Jakubéczyová, P. Hvizdoš, M. Selecká, Investigation of thin layers deposited by two PVD techniques on high speed steel produced by powder metallurgy, Appl Surf Sci 258 (2012) 5105–5110. https://doi.org/10.1016/j.apsusc.2012.01.138

[10] E. Franco, C.E. da Costa, J.C.G. Milan, S.A. Tsipas, E. Gordo, Multi-component boron and niobium coating on M2 high speed steel processed by powder metallurgy, Surf Coat Technol 384 (2020) 125306. https://doi.org/10.1016/j.surfcoat.2019.125306

[11] J.R. Davis (Ed.), Handbook of Thermal Spray Technology, ASM International, Materials Park, OH, 2004.

[12] L. Pawlowski, The science and engineering of thermal spray coatings, Wiley, Chichester, 2008.

[13] J.M. Miguel, J.M. Guilemany, S. Vizcaino, Tribological study of NiCrBSi coating obtained by different processes, Tribol Int 36 (2003) 181–187. https://doi.org/10.1016/S0301-679X(02)00144-5

[14] R. González, M. Cadenas, R. Fernández, J.L. Cortizo, E. Rodríguez, Wear behaviour of flame sprayed NiCrBSi coating remelted by flame or by laser, Wear 262 (2007) 301–307. https://doi.org/10.1016/j.wear.2006.05.009

[15] A. Eskandari, A. Shafyei, F. Sayyedan, M. Afsous, M. Adamzadeh, Investigating the microstructural, mechanical, and tribological properties of NiCrBSi HVOF and HP-HVOF coatings, J Mater Eng Perform 32 (2023) 1671–1682. https://doi.org/10.1007/s11665-022-07249-7

[16] R.C. Tucker, Introduction to thermal spray technology, ASM International, Materials Park, OH, 2013. https://doi.org/10.31399/asm.hb.v05a.a0005706

[17] H.L. Yu, W. Zhang, H.M. Wang, Y.L. Yin, X.C. Ji, K.B. Zhou, Comparison of surface and cross-sectional micro-nano mechanical properties of flame sprayed NiCrBSi coating, J Alloys Compd 672 (2016) 137–146. https://doi.org/10.1016/j.jallcom.2016.02.118

[18] P. Fauchais, G. Montavon, G. Bertrand, From powders to thermally sprayed coatings, J Therm Spray Technol 19 (2010) 56–80. https://doi.org/10.1007/s11666-009-9435-x

[19] J. Henao, C.A. Poblano-Salas, F. Vargas, A.L. Giraldo-Betancur, J. Corona-Castuera, O. Sotelo-Mazón, Principles and applications of thermal spray coatings, in: Advanced surface coating techniques for modern industrial applications, IGI Global, Hershey, PA, 2021, pp. 31–70.

[20] P. Fauchais, A. Vardelle, Thermal sprayed coatings used against corrosion and corrosive wear, Adv Plasma Spray Appl 10 (2012) 344–348.

[21] O. Altuntas, M. Ozer, G. Altuntas, A. Ozer, Investigation of the microstructure, hardness and electrical conductivity properties of Fe/Graphene compacts, Mater Sci Technol 39 (2023) 2670–2679. https://doi.org/10.1080/02670836.2023.221355

[22] H.K.D.H. Bhadeshia, Cementite, Int Mater Rev 65 (2020) 1–27. https://doi.org/10.1080/09506608.2018.156098

[23] M. Abid, H. Ben Abdelali, M. Kchaou, E. Bayraktar, M. Haboussi, Friction durability of anodized aluminum alloy 2017A under dry conditions, J Mater Eng Perform 33 (2024) 1457–1471. https://doi.org/10.1007/s11665-023-08065-3

[24] P.C. Angelo, R. Subramanian, B. Ravisankar, Powder metallurgy: science, technology and applications, PHI Learning, New Delhi, 2022.

[25] D. Qadir, R. Sharif, R. Nasir, A. Awad, H.A. Mannan, A review on coatings through thermal spraying, Chem Pap 78 (2024) 71–91. https://doi.org/10.1007/s11696-023-03089-4

[26] J. Rodríguez, A. Martín, R. Fernández, J.E. Fernández, An experimental study of the wear performance of NiCrBSi thermal spray coatings, Wear 255 (2003) 950–955. https://doi.org/10.1016/S0043-1648(03)00162-5

[27] J.F. Archard, Contact and rubbing of flat surfaces, J Appl Phys 24 (1953) 981–988. https://doi.org/10.1063/1.1721448

[28] S. Wei, L. Xu, Review on research progress of steel and iron wear-resistant materials, Acta Metall Sin 56 (2019) 523–538. https://doi.org/10.11900/0412.1961.2019.00370

[29] P.L. Hurricks, Some metallurgical factors controlling the adhesive and abrasive wear resistance of steels: a review, Wear 26 (1973) 285–304. https://doi.org/10.1016/0043-1648(73)90184-1

[30] Š. Houdková, E. Smazalová, M. Vostřák, J. Schubert, Properties of NiCrBSi coating, as sprayed and remelted by different technologies, Surf Coat Technol 253 (2014) 14–26. https://doi.org/10.1016/j.surfcoat.2014.05.009

[31] X. Sun, F. Li, Y. Li, J. Du, X. Qi, W. Cui, J. Niu, Enhancing the wear and high-temperature oxidation behavior of NiCrBSi coatings by collaboratively adding WC and Cr_3C_2, Surf Coat Technol 473 (2023) 129968. https://doi.org/10.1016/j.surfcoat.2023.129968